J. Mol. Biol. (1991) **218**, 847–858

Location of Ion-binding Sites in the Gramicidin Channel by X-ray Diffraction

Glenn A. Olah, Huey W. Huang†, Wenhan Liu‡ and Yili Wu

Physics Department, Rice University
Houston, TX 77251, U.S.A.

(Received 23 July 1990; accepted 3 January 1991)

We report the first X-ray diffraction on gramicidin in its membrane-active form by using uniformly aligned multilayer samples of membranes containing gramicidin and ions (Tl^+, K^+, Ba^{2+}, Mg^{2+} or without ions). From the difference electron density profiles, we found a pair of symmetrically located ion-binding sites for Tl^+ at 9·6(±0·3) Å and for Ba^{2+} at 13·0(±0·2) Å from the midpoint of the gramicidin channel. The location of Ba^{2+}-binding sites is near the ends of the channel, consistent with the experimental observation that divalent cations do not permeate but block the channel. The location of Tl^+-binding sites is somewhat of a surprise. It was generally thought that monovalent cations bind to the first turn of the helix from the mouth of the channel. (It is now generally accepted that the gramicidin channel is a cylindrical pore formed by two monomers, each a single-stranded $\beta^{6.3}$ helix and hydrogen-bonded head-to-head at their N termini.) But our experiment shows that the Tl^+-binding site is either near the bottom of or below the first helix turn.

1. Introduction

Gramicidin, a linear pentadecapeptide, is by far the most extensively studied membrane-active peptide that forms a transmembrane ion channel. It is now generally accepted that the gramicidin channel is a cylindrical pore formed by two monomers, each a single-stranded $\beta^{6.3}$ helix and hydrogen-bonded head-to-head at their N termini (Urry, 1985; Arseniev *et al.*, 1985). Recent nuclear magnetic resonance (n.m.r.§) studies have determined the helices to be right-handed (Arseniev *et al.*, 1985; Cornell *et al.*, 1988; Nicholson & Cross, 1989), but the contradiction with an earlier experimental evidence for left-handedness still needs to be resolved (Urry, 1985). The pore selectively facilitates the diffusion of monovalent cations across bilayer membranes, but does not transmit anions or divalent cations (Hladky & Haydon, 1984). There are extensive kinetic data describing the effect on the channel conductivities of a great number of variables, including amino acid variation, membrane variation, ion valence variation, cation variation, etc. (Hladky & Haydon, 1984; Andersen, 1984; Andersen *et al.*, 1987; Koeppe & Andersen, 1987). The relatively simple structure and the wealth of experimental data on its ion conductions make gramicidin an ideal model system for the study of the principles governing ion transport across lipid membranes. In particular, many molecular dynamics computations and simulations have been performed in an attempt to understand the detailed properties of the channel, such as the free energy profiles of ions, the hydrogen-bonding pattern of water, the ion and water motions, etc. (Mackay *et al.*, 1984; Pullman, 1987; Roux & Karplus, 1988; Jordan, 1988; Chiu *et al.*, 1989). Unfortunately, the lack of molecular data for comparison makes it difficult to evaluate these theoretical and computational results. One of the desirable molecular data is the location of the ion-binding sites, which, we believe, is the key to the ion selectivity.

That the channel has two monovalent cation-binding sites is consistent with known experimental data (Hladky & Haydon, 1984; Urry, 1985). Indeed, the binding constants for the first and second bindings of alkali metal cations have been estimated by

† Author to whom all correspondence should be addressed.

‡ On leave from Center for Fundamental Physics, University of Science & Technology of China, Hefei, Anhui, People's Republic of China.

§ Abbreviations used: n.m.r., nuclear magnetic resonance; c.d., circular dichroism; DLPC, dilauroylphosphatidylcholine; r.h., relative humidity; DMPC, dimyristoylphosphatidylcholine.

0022-2836/91/080847-12 $03.00/0

Tl^+-205 chemical shift studies (Hinton *et al.*, 1988) and n.m.r. relaxation methods (Urry, 1985). The bindings of divalent cations were first inferred from their ability to reduce the fluxes of monovalent ions (Bamberg & Läuger, 1977); further evidence was obtained from ^{13}C n.m.r. and ^{43}Ca n.m.r. relaxation studies (Urry, 1985; Urry *et al.*, 1988). However, the locations of all these binding sites are unknown. There was an earlier study on ion-induced chemical shifts of carbonyl carbon n.m.r. resonances, from which Urry and his collaborators concluded that two symmetric binding sites for monovalent cations are each localized between the Trp11 and Trp13 carbonyl groups of one monomer (Urry, 1985). But this same evidence was used also to conclude that the gramicidin helix is left-handed, a conclusion contradicted by more recent n.m.r. studies (Arseniev *et al.*, 1985; Cornell *et al.*, 1988; Nicholson & Cross, 1989).

Here, we report the use of uniformly aligned multilayer samples of membranes containing gramicidin and the X-ray diffraction measurement of such samples with and without ions (Tl^+, K^+, Ba^{2+}, Mg^{2+}). From the difference electron density profiles, we found a pair of symmetrically located ion-binding sites for Tl^+ at 9·6(±0·3) Å and for Ba^{2+} at 13·0(±0·2) Å (1 Å=0·1 nm) from the midpoint of the gramicidin channel. This is the first X-ray diffraction study on gramicidin in its membrane-active form and the first measurement indicating the length of this channel.

Since gramicidin is polymorphic, care must be taken in the preparation procedure to ensure that the peptide is in the channel state. It was Urry *et al.* (1979) who identified the channel state with a characteristic circular dichroism (c.d.) spectrum for gramicidin in lipid vesicles. The c.d. spectrum for channels aligned in parallel lipid multilayers was obtained by Huang & Olah (1987). For X-ray diffraction, we use multilayer samples held between two parallel plates. (We use beryllium on one side and fused silica on another for the ease of X-ray transmission and optical inspection, respectively.) The well-defined sample geometry allows the data reduction to be straightforward and rigorous. The experiment is described in Materials and Methods.

2. Materials and Methods

(a) *Materials and preparation of samples*

Gramicidin D (lot 21007) was purchased from ICN Biochemicals, Cleveland, OH. An amino acid analysis by high-pressure liquid chromatography showed it to be 77% gramicidin A, 5% gramicidin B and 18% gramicidin C; it was used without further purification. Dilauroylphosphatidylcholine (DLPC; lot 64F-8375) was purchased from Sigma Chemical Co., St. Louis, MO. All salts used were ultrahigh pure. All solvents used were of spectroscopic or high-pressure liquid chromatography grade and always filtered before use. Only 2MΩ distilled water was used.

Gramicidin and DLPC (~200 mg) in the molar ratio 1 : 10 were codissolved in benzene and lyophilized. Salt, in acetate form, was added in 1/3 portion at a time. During the addition of each 1/3 portion of salt, the water content was kept at 1 to 2 ml. The suspension was incubated in N_2 atmosphere for 18 h at 68°C. The suspension was also vortex mixed intermittently during incubation. The suspension was again lyophilized and the next 1/3 portion of salt added. The process was repeated 3 times until the desired salt concentration was attained. The final lyophilized fluffy white powder was then exposed to N_2 gas with 100% relative humidity (r.h.) at ~23°C. In about a week, the mixture turned into a clear gel, ready to be aligned into multilayers. The lipid under this condition is in the L_α liquid crystalline phase (Huang & Olah, 1987). This procedure was sufficient to totally mix the salt into the sample batch as well as induce the gramicidin into the channel state. Final salt concentrations for 5 different batches had cation/peptide/lipid molar ratios as follows: 0 : 1 : 10 (salt-free sample), 1 : 1 : 10 (Tl^+ sample), 1·5 : 1 : 10 (K^+ sample), 1 : 1 : 10 (Ba^{2+} sample), 1 : 1 : 10 (Mg^{2+} sample). The Tl^+ and K^+ concentrations were high enough to ensure that approx. 80% of the gramicidin ion-binding sites were bound during the final incubation, assuming the binding constants given by Hinton *et al.* (1988). The binding constants for divalent ions are unknown.

(b) *Examination by circular dichroism*

A small amount of each sample batch was removed to prepare a vesicle sample for c.d. measurement. The allotment was diluted with water or a salt solution such that the DLPC concentrations were approximately 4 mg/ml: c.d. was measured immediately after the mixture was sonicated for 30 min as described by Huang & Olah (1987) and Wu *et al.* (1990). The spectra are shown in Fig. 1(a): they are characteristic of the channel state (Urry *et al.*, 1979). The technique for preparing uniformly aligned, defect-free lipid multilayers has been described (Huang & Olah, 1987; Olah & Huang, 1988). For the measurement of oriented c.d. the multilayer samples were sandwiched between 2 silica plates (for details, see Wu *et al.*, 1990). The oriented c.d. measured with light incident normal to the plane of multilayers are given in Fig. 1(b). Since the same spectra can be obtained by drying vesicle samples on a silica plate, we have proven that the gramicidin in our multilayer samples is indeed in the channel state.

(c) *X-ray diffraction*

Multilayer samples for diffraction studies were aligned between a polished Be plate (262 μm × 17 mm diam. or 314 μm × 10 mm diam.) and a silica plate without a spacer. The thicknesses of the multilayers were about 10 μm. The samples were in contact with the atmosphere, so their water contents were controllable by regulating the humidity of the sample chamber. The alignment of a sample was examined from the silica side by using a reflection polarizing microscope (Huang & Olah, 1987).

The aligned sample was kept in a humidity chamber with X-ray windows, initially at 100% r.h. at 18·0(±0·5)°C. Bragg diffraction was measured from the Be side using $\theta-2\theta$ geometry on an AFC-5 Rigaku 4-circle diffractometer with a 12 kW rotating (Cu) anode X-ray generator at the Howard Hughes Medical Institute, Baylor College of Medicine. The humidity control in the chamber was such that the sample would slowly lose water so the lamellar spacing (i.e. the repeat distance) decreased approximately 5 Å in 48 h (the initial lamellar spacing was typically about 46 Å). The $\theta-2\theta$ scans were repeated approx. every 70 min. Since the lamellar

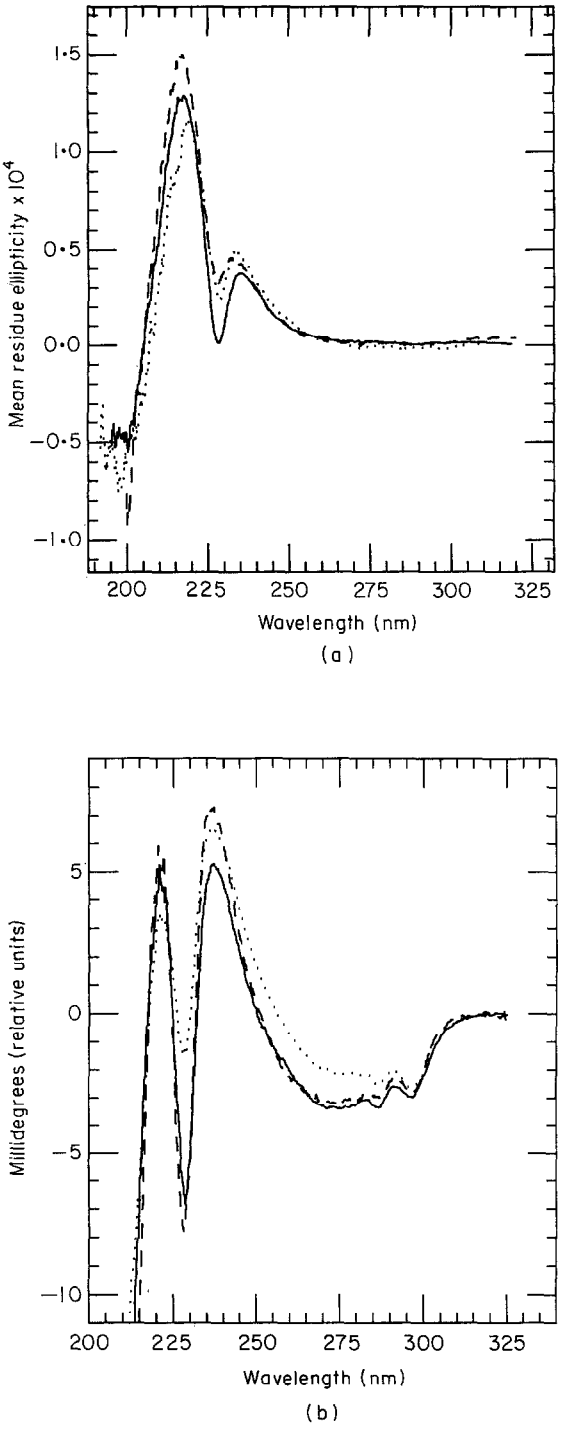

Figure 1. (a) Circular dichroism (c.d.) of gramicidin in DLPC (molar ratio 1 : 10) vesicles with 100 mM-thallium acetate (dotted line), with 30 mM-barium acetate (broken line) and without salt (continuous line). (b) Oriented c.d. of gramicidin/DLPC multilayers with thallium acetate (molar ratios 1 : 10 : 1; dotted line), with barium acetate (molar ratios 1 : 10 : 1; broken line) and without salt (molar ratio 1 : 10; continuous line), measured with light incident normal to the plane of the stacked lipid bilayers; the gramicidin/DLPC multilayer samples with potassium acetate (molar ratios 1 : 10 : 1·5) and with magnesium acetate (molar ratios 1 : 10 : 1) have similar spectra (not shown). Compared with the c.d. of different molecular conformations (Urry, 1985), these spectra show only small perturbations caused by ion bindings.

spacing never decreased more than 1% during 3 consecutive scans, data of 3 consecutive scans were averaged to represent 1 lamellar spacing.

Typically, 8 Bragg orders were recorded (Fig. 2), corresponding to 5 Å (approx. lamellar spacing/8) resolution. This is a very high resolution for DLPC membranes in the L_α liquid-crystalline phase. By the same method, 13

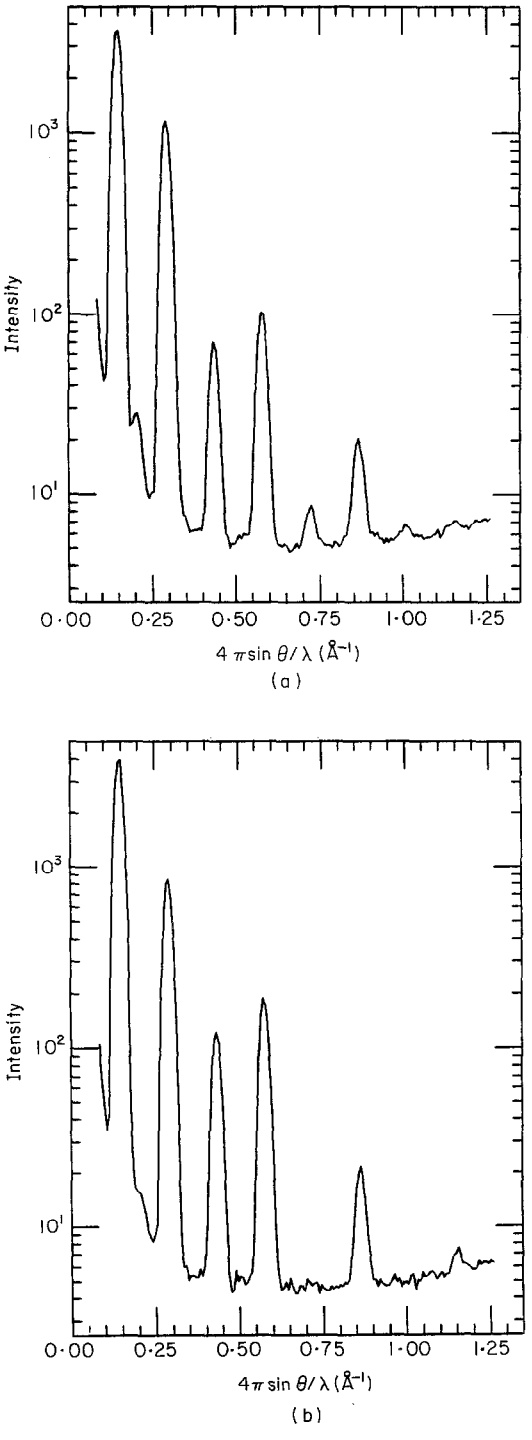

Figure 2. Our typical X-ray diffraction patterns of gramicidin/DLPC multilayers: (a) with thallium acetate and (b) without salt. Eight Bragg orders were recorded. The lamellar spacings for both patterns were 43·4 Å.

Bragg orders were recorded for dimyristoylphosphatidylcholine (DMPC)/cholesterol multilayers in the L_α phase (Olah, 1990), which corresponds to the highest resolution ever recorded for such systems (Franks & Lieb, 1979).

(d) *Data reduction*

The procedure of data reduction is similar to that of Franks & Lieb (1979), including (1) background subtraction, (2) corrections for polarization, the Lorentz factor, scattering volume, Be and specimen absorption, the second harmonic (which becomes significant due to the absorption by the Be plate) and the atomic scattering factors, and (3) the detector vertical slit correction for beam divergence and sample mosaic (0·3° to 0·5°: Saxena & Schoenborn 1977). To test our experimental procedure and data analysis, we reproduced Franks & Lieb's electron density profiles for DMPC/cholesterol (Olah, 1990).

The relative phases of Bragg reflections were determined from the water swelling data. For a given lamellar spacing D, the reflection intensities were scaled to satisfy Blaurock's scaling relation (Blaurock, 1971):

$$\sum_h I(h) = D/D_{\min}, \qquad (1)$$

where $I(h)$ is the scaled intensity for the Bragg reflection of order h, $D_{\min}$ is a constant usually taken as the minimum lamellar spacing in the swelling series for each type of sample. Amplitudes, i.e. the square-roots of the scaled intensities, are plotted in Figs 3 and 4 as a function of the reciprocal lattice vector $2\pi h/D$ (or $4\pi\sin\theta/\lambda$). The plates (which are either 0 or π due to the centrosymmetry of bilayer membranes) were chosen so that the data points fall on a single smooth curve and appropriately satisfy the minimum wavelength principle (Perutz, 1954). These phase assignments produce electron density profiles that essentially remain constant during the swelling series (see below). Alternative phase assignments were considered and rejected; they produce electron density profiles that are either physically implausible or changing with hydration in a complicated fashion (Torbet & Wilkins, 1976; examples and discussions are given in the Appendix). We extensively tested the reproducibility of our data. Both sample preparation and X-ray measurement were repeated at least 3 times for each type of sample; data from different runs are seen to overlap each other (Figs 3 and 4).

3. Results

(a) *Location of Tl^+-binding sites*

The structure factors are Fourier transformed to obtain the scattering density profiles ρ_{sc}. This is related to the true electron density ρ by $\rho = c\rho_{sc} + b$. The two constants b and c can be determined, if we know the composition of the sample, the molecular areas (along the plane of membrane) of lipid and gramicidin, and the value of ρ at one point, e.g. the density minimum at the bilayer center. Because the structures of the three samples (Tl^+, K^+ and salt-free) are nearly the same, the position of the ion-binding sites that will be determined from the difference profiles is rather insensitive to the values of b and c. The following numbers are used to evaluate the electron density of a unit cell consisting of a gramicidin dimer, 20 DLPC molecules and their associated water and salt molecules.

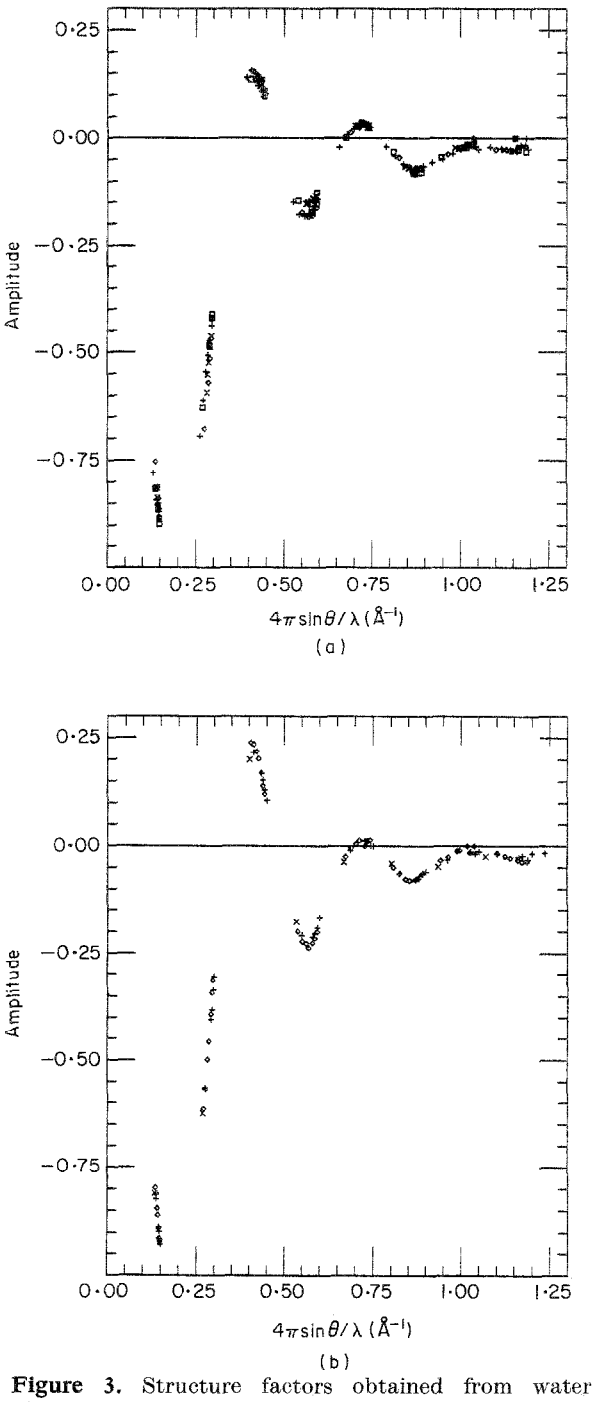

Figure 3. Structure factors obtained from water swelling experiments, with their amplitudes scaled as described in the text and their phases chosen so that the data points fall on a single smooth curve ((a) 4 different Tl^+ samples; (b) 3 different salt-free samples).

(1) The number of electrons per molecule of DLPC and gramicidin is 342 and 1011, respectively.

(2) The volume per molecule of DLPC in the L_α phase, gramicidin (crystal) and water is 992 Å^3, 3096 Å^3 (gramicidin without ions), 3259 Å^3 (gramicidin with CsCl), and 29·9 Å^3, respectively. The volume for DLPC was taken from the data of Knoll

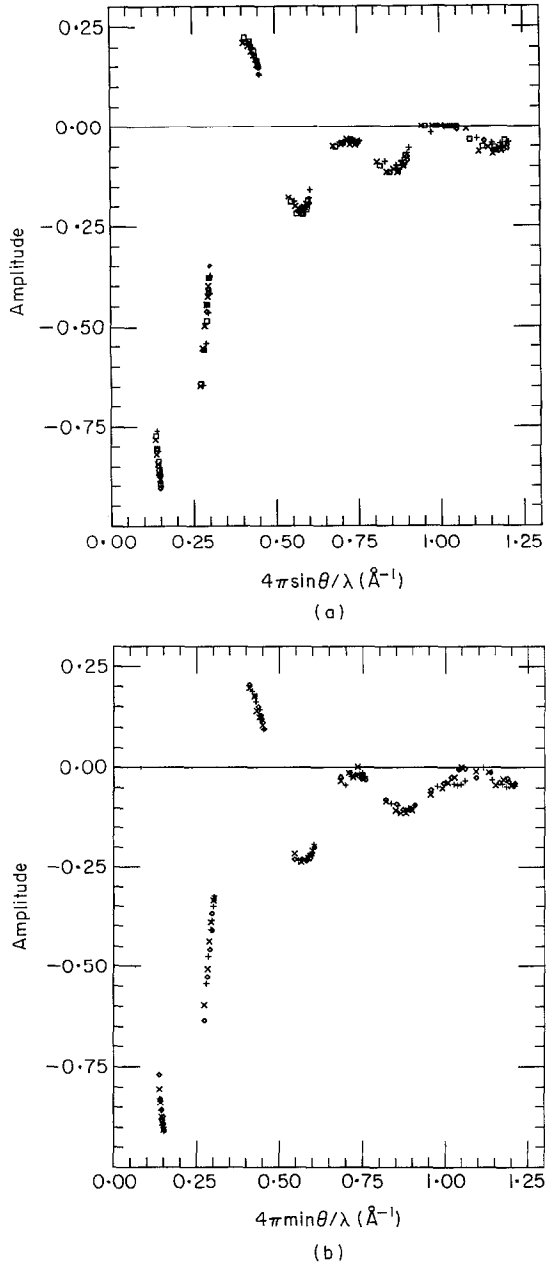

Figure 4. Same as Fig. 3 for (a) 4 different Ba^{2+} samples and (b) 3 different Mg^{2+} samples.

(1981). The volume for gramicidin without ions was taken from Langs (1988) and gramicidin with CsCl from Wallace & Ravikumar (1988).

(3) The smallest lamellar spacing in the swelling experiment is about 41·5 Å. We assume that, under this condition, each DLPC has three water molecules associated with it (8% (w/w) water). The cross-section for the DLPC molecule is then approximately $2(992\ Å^3+3(29{\cdot}9\ Å^3))/41{\cdot}5\ Å = 52{\cdot}1\ Å^2$.

(4) The length of the gramicidin dimer is about 26 Å (Koeppe & Kimura, 1984). Assuming the volume of gramicidin in membrane is about the same as in crystals, the cross-section of the gramicidin dimer is about 250 $Å^2$. The cross-sectional area (parallel to the plane of membrane) per unit cell is then $10\times52\ Å^2+250\ Å^2=770\ Å^2$.

(5) We assume that there are ten water molecules inside the gramicidin channel. Also, water fills all the space outside the mouth of the channel.

(6) From the density measurements of lethicin bilayers (54 $Å^3/CH_3$ in the L_α phase (Nagle & Wilkinson, 1978) gives 0·17 $e/Å^3$ for the terminal methyl groups) and the electron density of gramicidin (0·34 $e/Å^3$), we estimated the electron density at the center of the bilayer to be 0·22 e/A^3. This value assumes that there are no ions in the central region of the channel (see below).

Thus, the total number of electrons in one unit cell of lamellar spacing D is given by:

gramicidin/DLPC (1 : 10):
$$10{,}858+258(D-41{\cdot}5), \quad (2)$$

Tl^+/gramicidin/DLPC (1 : 1 : 10):
$$11{,}082+258(D-41{\cdot}5), \quad (3)$$

K^+/gramicidin/DLPC (1·5 : 1 : 10):
$$11{,}008+258(D-41{\cdot}5), \quad (4)$$

Ba^{2+}/gramicidin/DLPC (1 : 1 : 10):
$$11{,}094+258(D-41{\cdot}5), \quad (5)$$

Mg^{2+}/gramicidin/DLPC (1 : 1 : 10):
$$11{,}006+258(D-41{\cdot}5), \quad (6)$$

where, for example in equation (2), 10,858 is 7440 (20 [DLPC+3 water molecules]) plus 2122 (1 gramicidin dimer $+10\ H_2O$) plus $10(41{\cdot}5-26)\times250/29{\cdot}9=1296$ (water filling the space outside the mouth of the channel); the second term is the hydration water between lipid bilayers $10(D-41{\cdot}5)\times770/29{\cdot}9$. b and c for each sample were obtained by using these equations and the electron density at the bilayer center. We have varied the cross-sectional area of unit cell and the value of ρ at the bilayer center by 10% from the above values and found that it did not change the position of the ion-binding sites determined below. Figure 5 shows the normalized electron density profiles ρ of the gramicidin/DLPC bilayers with Tl^+, with K^+ and without ions all at the lamellar spacing 43·4 Å. The central regions of the bilayers for the three samples are the same within error; therefore, we take this to indicate that there are no ions in this region and also to justify our choice of the same ρ minimum for all samples. Figure 6 shows that the electron density profile of the Tl^+ sample essentially remains the same during a swelling series. This is true also for the K^+ and salt-free samples (not shown).

The difference electron density profile is obtained from two ρ profiles having the same lamellar spacing D. The top two curves in Figure 7, are two examples of the difference profile, $\rho(Tl^+$ sample$)-\rho$(salt-free sample), obtained from data of lamellar spacings 42·4 Å and 43·4 Å. Each profile

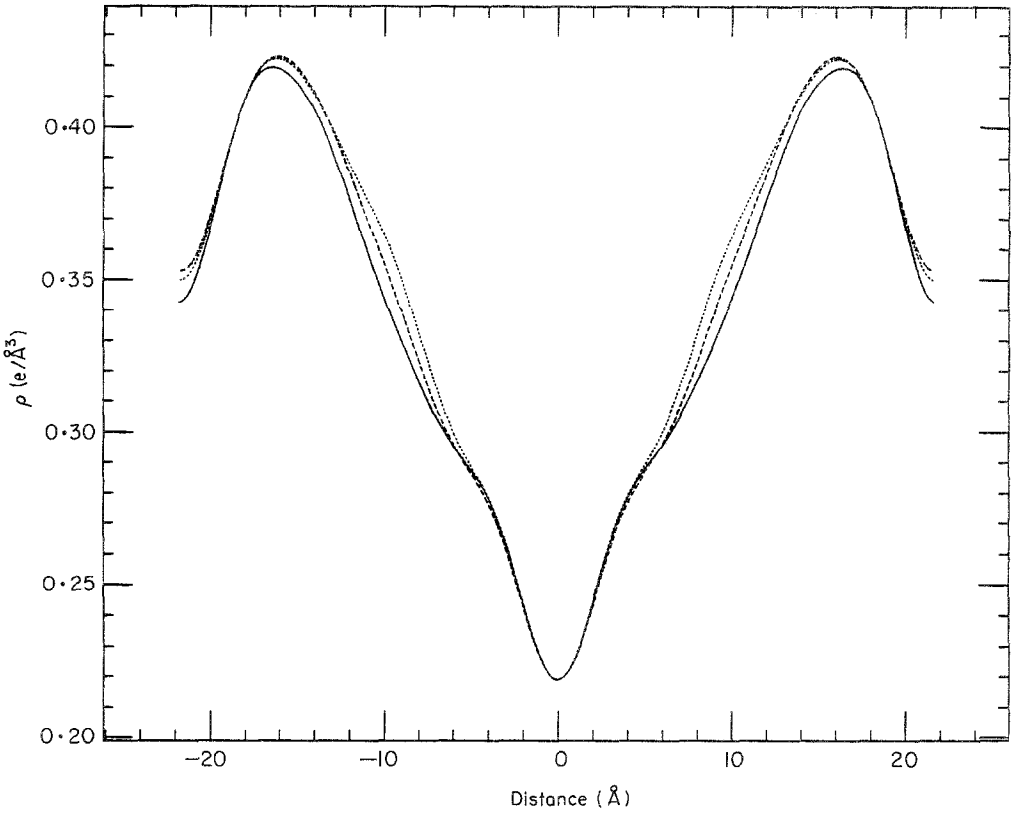

Figure 5. Normalized electron density profiles of gramicidin/DLPC bilayers with Tl^+ (dotted line), with K^+ (broken line) and without salt (continuous line), obtained from the structure factors of lamellar spacing 43·4 Å.

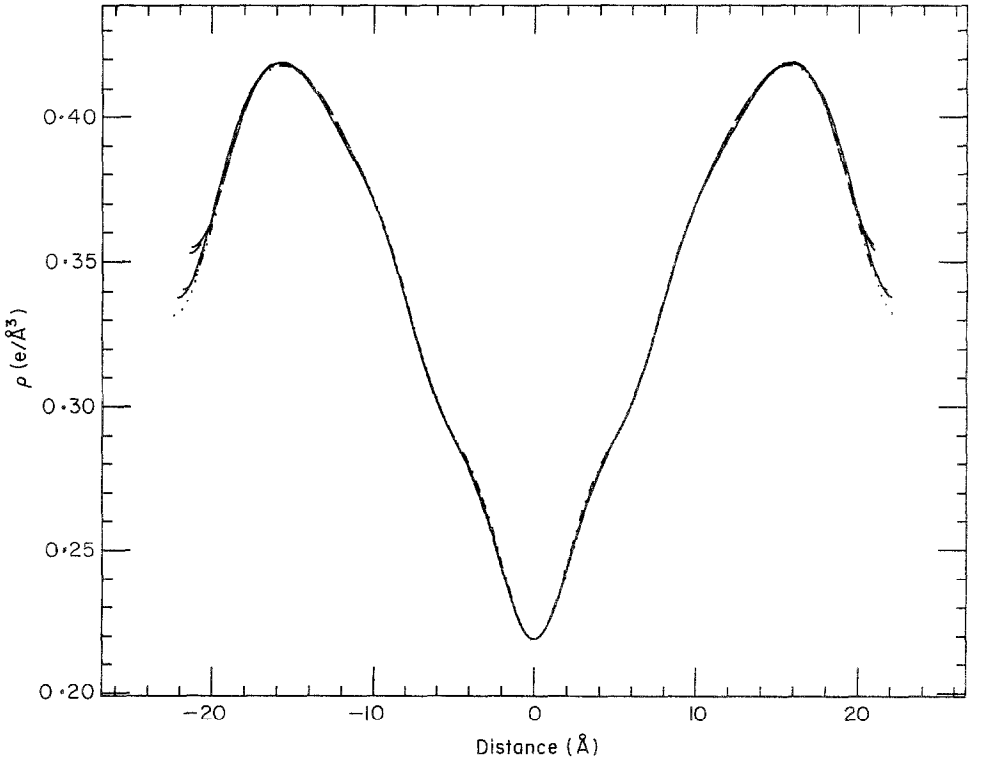

Figure 6. Normalized electron density profiles of gramicidin/DLPC bilayers with Tl^+ during a swelling experiment. The profiles of 5 different lamellar spacings are shown: D=44·8 Å, 44·3 Å, 43·6 Å, 42·7 Å and 42·5 Å.

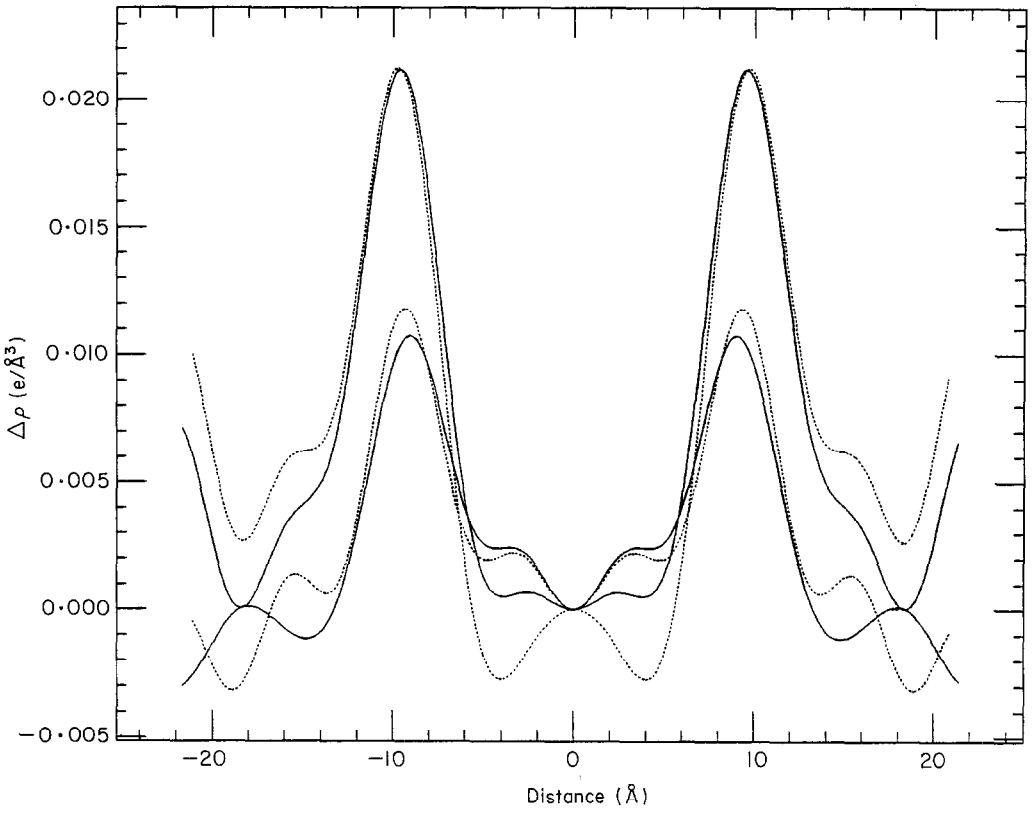

Figure 7. Difference electron density profiles. The top 2 are ρ(thallium sample)$-\rho$(salt-free sample). The bottom 2 are ρ(thallium sample)$-\rho$(potassium sample). Continuous lines are obtained from the profiles of lamellar spacings 43·4 Å; dotted lines from lamellar spacing 42·4 Å.

represents a measurement of the electron density distribution of Tl^+. The distribution indicates that the majority of Tl^+ ions are bound inside the channels, as one would expect from the binding constant (Hinton *et al.*, 1988); each channel binds two Tl^+, according to the ion to gramicidin ratio. The peak positions indicate the locations of the Tl^+-binding sites; the width of the peak represents the resolution of diffraction, approximately 5 Å. We also calculated $\rho(Tl^+$ sample$)-\rho(K^+$ sample), the bottom two curves in Figure 7. Since K^+ has a relatively small binding constant (Hinton *et al.*, 1988), excessive amount of K^+ in the sample was considered necessary to ensure that the majority of the binding sites are occupied. As a result, about one-third or more of K^+ are outside the channel. Figure 8 shows an example of the difference profile $\rho(K^+$ sample$)-\rho$(salt-free sample). The distributions inside and outside the channel overlap, causing the apparent position of the inside peak to shift toward outside. Consequently, the peak positions of Tl^+ obtained from $\rho(Tl^+$ sample$)-\rho(K^+$ sample) are shifted slightly toward the center. Due to its unfavorable signal-to-noise ratio, the K^+ distribution profile was not analyzed further. The location of Tl^+-binding sites is determined solely from the difference profiles, $\rho(Tl^+$ sample$)-\rho$(salt-free sample).

The locations of the two binding sites are symmetric with respect to the center. This is proven by the fact that, while both binding sites are occupied, there is only one sharp peak on each side of the center. (Because of the way the samples were prepared, if 2 sites were asymmetric, 2 peaks would appear on each side.) Figure 9(a) compiles the peak positions of the difference profiles, $\rho(Tl^+$ sample$)-\rho$(salt-free sample), obtained from using four different Tl^+ samples and three different salt-free samples, evaluated at various lamellar spacings. The distribution represents the fluctuation of error. From the average and the dispersion of this histogram, Tl^+-binding sites are determined to be at 9·6($\pm$0·3) Å from the midpoint of the channel. Figure 9(b) shows the corresponding peak height dispersion (the widths are all about the same). The peak areas indicate that 85($\pm$13)% of Tl^+ are bound to the sites.

(b) *Locations of Ba^{2+}-binding sites*

The electron density profiles are normalized as above. Figure 10 shows the profiles of the gramicidin/DLPC bilayers with Ba^{2+} and Mg^{2+} at lamellar spacing 42·8 Å. The central regions of the two profiles are essentially the same, but they are substantially different from those of the monovalent cation samples and that of the salt-free sample; the last three are essentially the same in the central

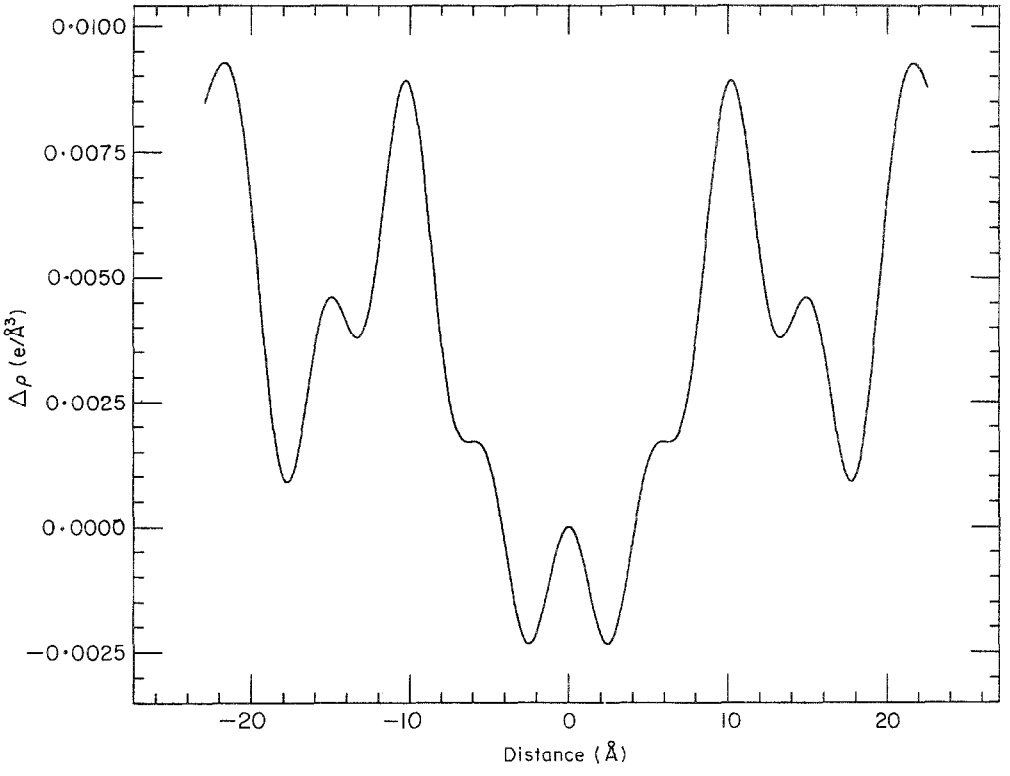

Figure 8. A difference electron density profile ρ(potassium sample)$-\rho$(salt-free sample).

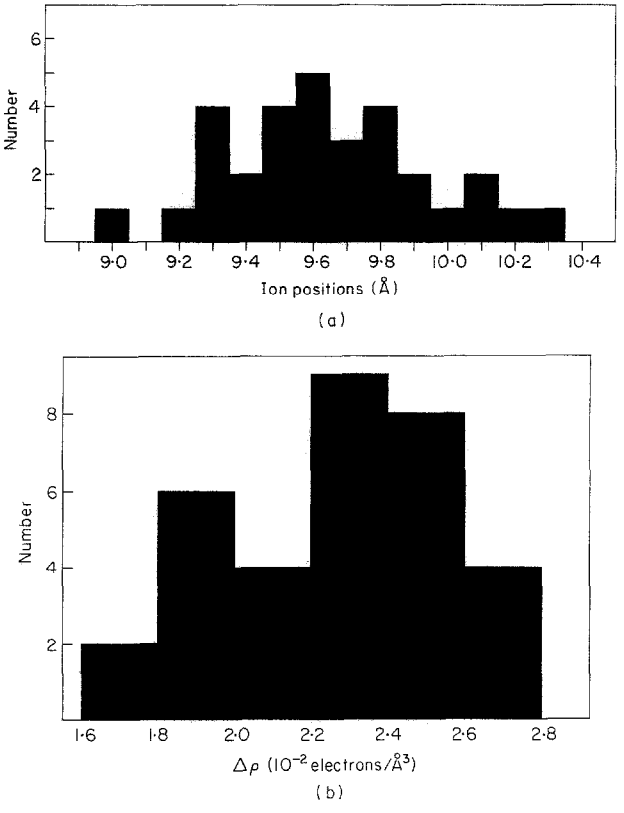

Figure 9. (a) A histogram of the peak positions of the difference profiles, ρ(thallium sample)$-\rho$(salt-free sample): 31 difference profiles were obtained from 4 thallium samples and 3 salt-free samples, evaluated at various lamellar spacings. (b) A histogram of the corresponding peak height dispersion.

region (Figs 5 and 6). For this reason, we subtract the Mg^{2+} profile, but not the salt-free profile, from the Ba^{2+} profile. However, unlike the case of $\rho(Tl^+$ sample$)-\rho(K^+$ sample), where there are excessive K ions, we have equal number of Ba and Mg ions in the respective samples. And, again, the electron density profiles of both the Ba^{2+} and Mg^{2+} samples remain essentially constant in swelling series (not shown).

Figure 11 shows two examples of the difference profile, $\rho(Ba^{2+}$ sample$)-\rho(Mg^{2+}$ sample), obtained from data of lamellar spacings 42·8 Å and 44·4 Å. The sharp peaks indicate that Ba^{2+} ions are well localized. Figure 12(a) compiles the peak positions of the difference profiles, $\rho(Ba^{2+}$ sample$)-\rho(Mg^{2+}$ sample), obtained from using four different Ba^{2+} samples and three different Mg^{2+} samples, evaluated at various lamellar spacings. From the average and the dispersion of the histogram, two symmetric Ba^{2+} binding sites are determined to be at 13·0($\pm$0·2)Å from the channel midpoint. Figure 12(b) shows the corresponding peak height dispersion. The peak areas indicate that 82($\pm$17)% of Ba ions are bound to the sites.

4. Discussion

Gramicidin in the conformation defined by the c.d. studies shown in Figure 1(a) has been examined for its helical sense. It was first determined to be left-handed by ^{13}C n.m.r. chemical shift measurements (Urry *et al.*, 1979; Urry, 1985), but a more recent two-dimensional ^1H-n.m.r. study determined it to be right-handed (Arseniev *et al.*, 1985; see also

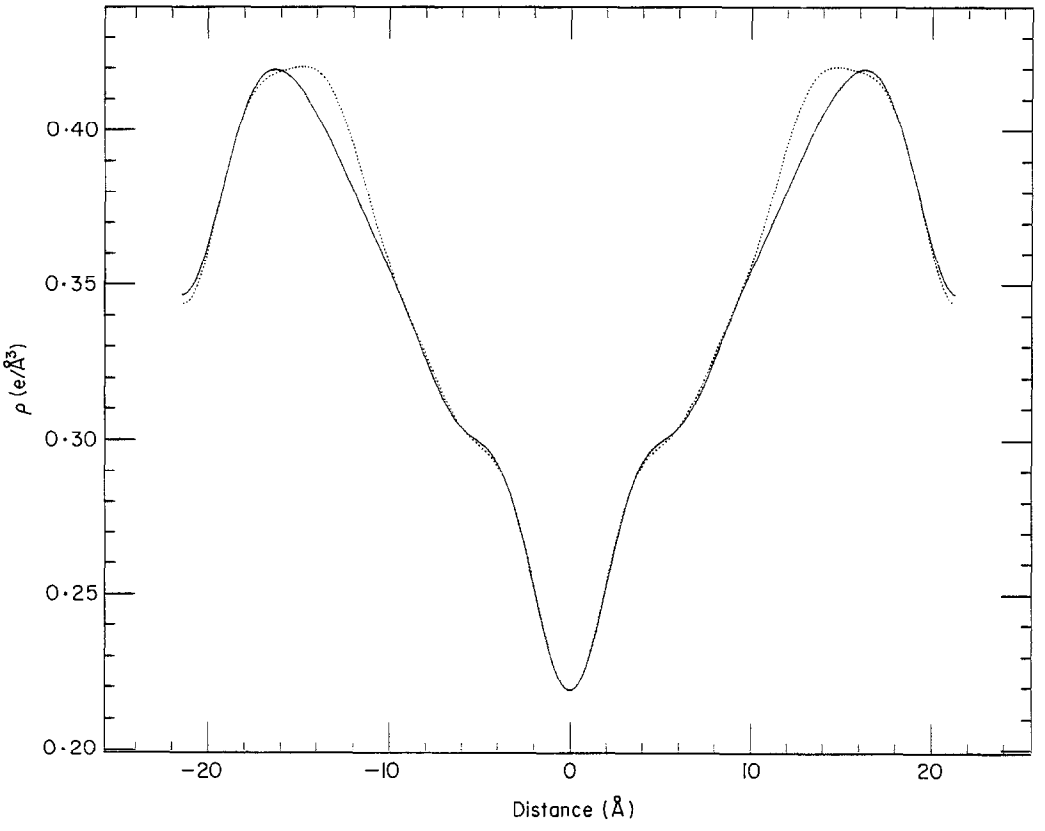

Figure 10. Normalized electron density profiles of gramicidin/DLPC bilayers with Ba^{2+} (dotted line) and with Mg^{2+} (continuous line), obtained from the structure factors of lamellar spacing 42·8 Å.

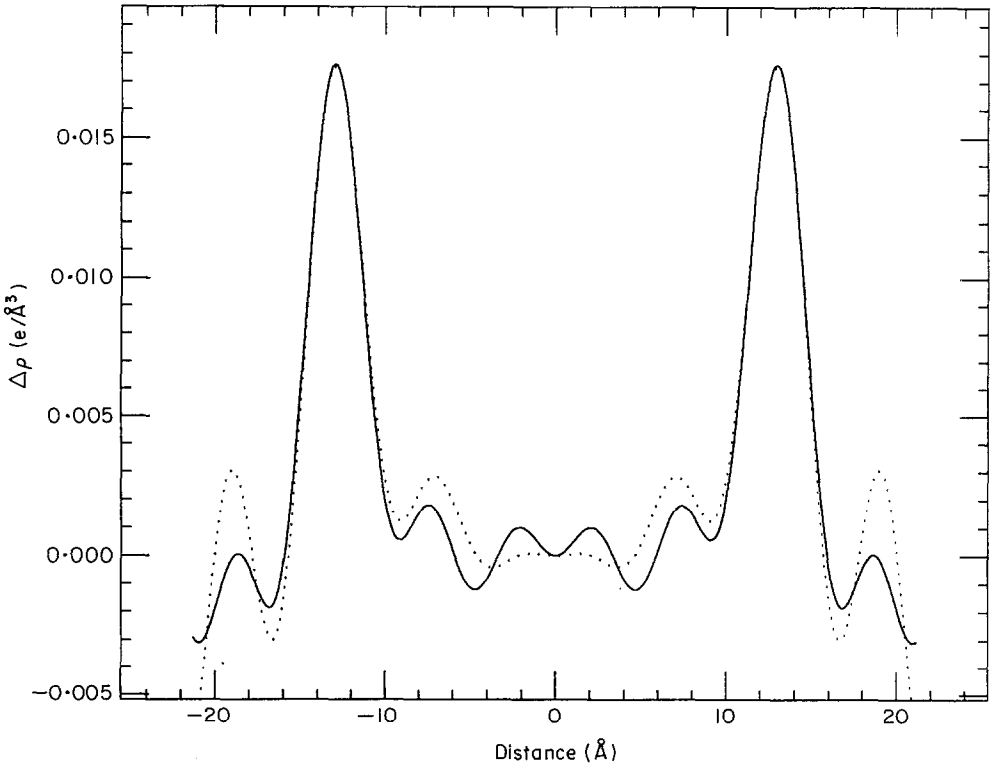

Figure 11. Difference electron density profiles ρ(barium sample)$-\rho$(magnesium sample) at lamellar spacings 42·8 Å and 44·4 Å.

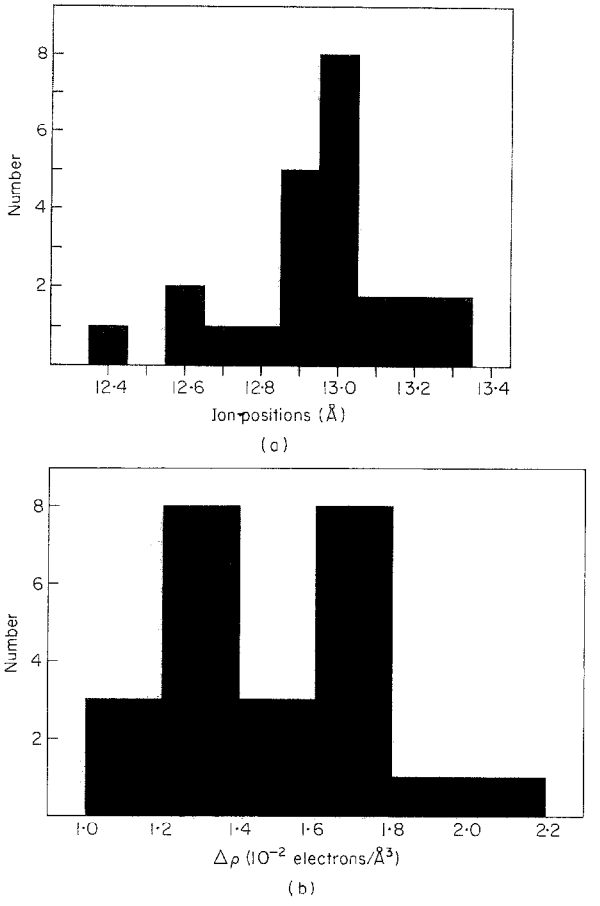

Figure 12. (a) A histogram of the peak positions of the difference profiles, ρ(barium sample)$-\rho$(magnesium sample): 24 difference profiles were obtained from 4 barium samples and 3 magnesium samples, evaluated at various lamellar spacings. (b) A histogram of the corresponding peak height dispersion.

Cornell *et al.*, 1988 and Nicholson & Cross, 1989). In either case, it is quite natural to suggest that the ion-binding site is on the first turn of the helix from the mouth (Hladky & Haydon, 1984; Jordan, 1988). At the mouth of the channel, the last six carbonyl groups (D-Leu10 to L-Trp15) are hydrogen-bonded only to one neighbor; three unbonded carbonyl oxygen atoms (Leu10, Leu12, and Leu14 in the case of a right-handed helix, Trp11, Trp13 and Trp15 in the case of a left-handed) are pointing toward the outside of the channel, as is the hydroxyl group of the ethanol amine tail. The surprising finding of our experiment is that the Tl^+-binding site, at 9·6(±0·3) Å from the channel midpoint, is either near the bottom of or below the first helix turn (Koeppe & Kimura, 1984).

On the other hand, Ba ions, at 13·0(±0·2) Å from the channel midpoint, apparently bind to the channel near the ends. This location is consistent with the experimental observation that divalent cations do not permeate but block the channel (Bamberg & Läuger, 1977). Thus, we suggest that the separation between two opposite Ba^{2+}-binding sites, i.e. 26·0(±0·4) Å, is a good measure for the length of the gramicidin channel. The molecular basis for the selectivity against divalent cations is probably straightforward. The gramicidin channel is a pore of 4 Å in diameter separated from a hydrophobic dielectric medium only by a single layer of polypeptide backbone. A cation entering the channel must overcome its dehydration energy (Pullman, 1987) and encounters an image potential (Parsegian, 1969). Both the dehydration energy and the image potential are greater for divalent cations than for monovalent cations.

Our diffraction experiment also reveals some interesting properties of the membrane–gramicidin interactions. It is well known that a pure lipid bilayer changes its thickness with hydration (Luzzati, 1968; Levine & Wilkins, 1971; Torbet & Wilkins, 1976; McIntosh, 1978; Olah, 1990). But if the bilayers contain cholesterol at a sufficiently high concentration, this effect is absent (Rand & Pangborn, 1973; Franks, 1976; Worcester & Franks, 1976; McIntosh, 1978; Olah, 1990), and there is a tendency for the hydrocarbon thickness of the bilayer to match that of a pair of cholesterol molecules (Franks & Lieb, 1979). For this reason, cholesterol is called a membrane "thickness buffer". Gramicidin is very likely another membrane thickness buffer. In all our samples, the phosphate peak-to-peak distances across the DLPC/gramicidin bilayers are virtually identical at 32·1 Å, irrespective of the degree of hydration. The assumption that the local hydrocarbon thickness of a lipid bilayer tends to match that of an embedded gramicidin channel was the basis of previous studies on the effect of membrane thickness on the gramicidin channel lifetime (Elliott *et al.*, 1983; Hladky & Haydon, 1984; Huang, 1986).

Appendix
Phase Determination

The swelling method for phase determination has been discussed extensively (Perutz, 1954; Blaurock, 1971; Torbet & Wilkins; 1976; Franks & Lieb, 1979). Because of the absence of the zeroth order peak (which makes the Shannon construction (Shannon, 1949) imprecise) and because the range of swelling is limited, the phase assignment is not without ambiguity even if the bilayer structure remains constant during swelling. In other words, there may be more than one apparent way to fit all amplitudes on a single smooth curve, as in the cases of Figures 3 and 4. It is then necessary to examine the alternative phase assignments and compare the consequences with the result presented in the text. Two examples are shown in Figures 13 and 14, in which the eighth orders of Figure 3(a) and 4(a) are changed to positive. The electron density profiles are then obtained by the same procedure described in the main text; the resulting bilayer structures change with hydration in non-systematic ways (Fig. 14). We found that all alternative phase assignments for

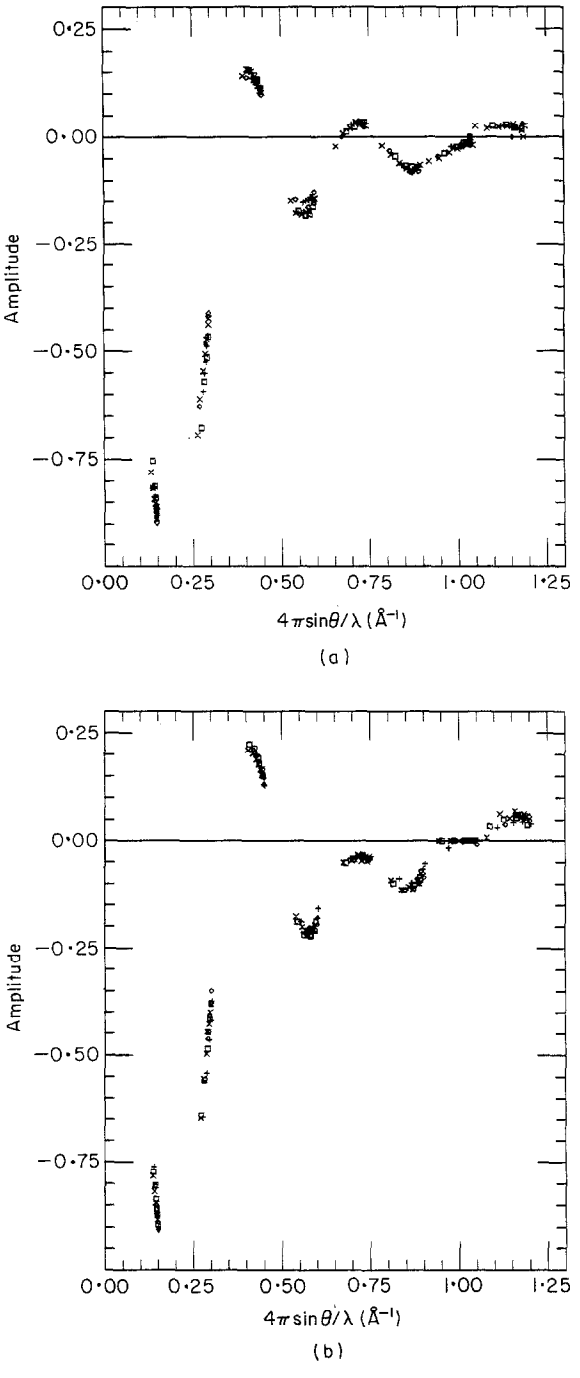

Figure 13. Two examples of alternative phase assignments that seem to fit all amplitudes on a single smooth curve. (a) The 8th order changes its sign from Fig. 3(a). (b) The 8th order changes its sign from Fig. 4(a).

Figures 3 and 4 (that seem to fit all amplitudes in a single smooth curve) are undesirable for one or both of two reasons: (1) structures are physically implausible; (2) bilayer structures change with hydration in complicated ways.

We emphasize that we are comparing chemically similar bilayer systems. Between the Tl^+ and K^+ systems or between the Ba^{2+} and Mg^{2+} systems, it

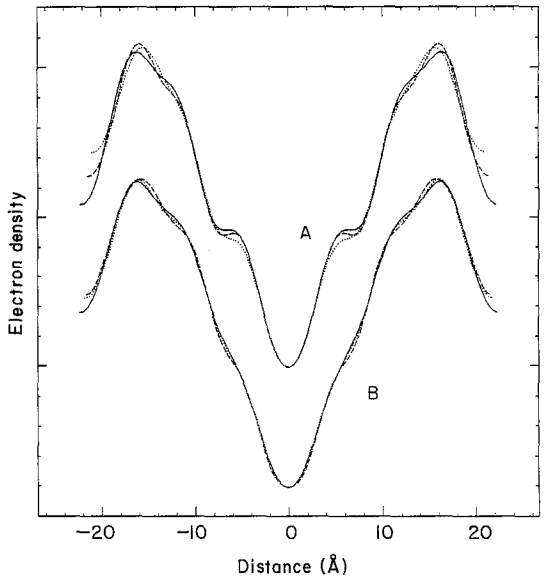

Figure 14. The normalized electron density profiles of the phase assignments shown in Fig. 13, obtained by the procedure described in the text. The bilayer structures change with hydration in non-systematic ways. Curve A corresponds to Fig. 13 (a) and curve B corresponds to Fig. 13(b).

is reasonable to expect the profiles of the two bilayers to be the same except where the ions are located. Figures 5 and 10 show that this is indeed the case. The difference profiles in Figures 7 and 11 give a single, well-defined peak on each half of the channel. Other difference profiles obtained from alternative phase assignments do not give such well-defined peaks. Thus, our phase assignments were chosen based on the well-established assumption that a simple and unique solution is more likely to be correct than complicated alternative solutions and a structure that remains constant with hydration is physically plausible (Torbet & Wilkins, 1976).

We are indebted to Professor Florante A. Quiocho, who made this experiment possible by letting us use the X-ray facilities in his laboratory. We thank Olaf Andersen, Si Moss and George Phillips for discussions. This research was supported in part by the Office of Naval Research (grant N00014-90-J-1020), the Robert A. Welch Foundation, and the NIH Biophysics Training grant GM 08280.

References

Andersen, O. S. (1984). *Annu. Rev. Physiol.* **46**, 531–548.

Andersen, O. S., Koeppe, R. E., II, Durkin, J. T. & Mazet, J.-L. (1987). In *Ion Transport through Membranes* (Yagi, K. & Pullman, B., eds), pp. 295–314, Academic Press, New York.

Arseniev, A. S., Barsukov, I. L., Bystrov, V. F., Lomize, A. L. & Ovchinnikov, Yu. A. (1985). *FEBS Letters*, **186**, 168–174.

Bamberg, E. & Läuger, P. (1977). *J. Membr. Biol.* **35**, 351–375.
Blaurock, A. E. (1971). *J. Mol. Biol.* **56**, 35–52.
Chiu, S. W., Subramaniam, S., Jakobsson, E. & McCammon, J. A. (1989). *Biophys. J.* **56**, 253–261.
Cornell, B. A., Separovic, F., Baldassi, A. J. & Smith, R. (1988). *Biophys. J.* **53**, 67–76.
Elliott, J. R., Needham, D., Dilger, J. P. & Haydon, D. A. (1983). *Biochim. Biophys. Acta*, **557**, 95–103.
Franks, N. P. (1976). *J. Mol. Biol.* **100**, 345–358.
Franks, N. P. & Lieb, W. R. (1979). *J. Mol. Biol.* **133**, 469–500.
Hinton, J. F., Fernandez, J. Q., Shungu, D. C., Whaley, W. L., Koeppe, R. E. & Millett, F. S. (1988). *Biophys. J.* **54**, 527–533.
Hladky, S. B. & Haydon, D. A., (1984). In *Current Topics in Membranes and Transport* (Stein, W. D., ed.), vol. 21, pp. 327–372, Academic Press, New York.
Huang, H. W. (1986). *Biophys. J.* **50**, 1061–1070.
Huang, H. W. & Olah, G. A. (1987). *Biophys. J.* **51**, 989–992.
Jordan, P. C. (1988). In *Current Topics in Membranes and Transport* (Agnew, W. S., Claudio, T. & Sigworth, F. J., eds), vol. 33, pp. 91–111, Academic Press, New York.
Knoll, W. (1981). *Chem. Phys. Lipids*, **28**, 337–345.
Koeppe, R. E., II & Andersen, O. S. (1987). In *Proteins: Structure and Function* (L'Italien, J. J., ed.), pp. 623–628, Plenum Press, New York.
Koeppe, R. E., II & Kimura, M. (1984). *Biopolymers*, **23**, 23–38.
Langs, D. A. (1988). *Science*, **241**, 188–191.
Levine, Y. K. & Wilkins, M. H. F. (1971). *Nature New Biol.* **230**, 69–72.
Luzzati, V. (1968). In *Biological Membranes* (Chapman, D., ed.), pp. 71–123, Academic Press, London.
Mackay, D. H. J., Berens, P. H., Wilson, K. R. & Hagler, A. T. (1984). *Biophys. J.* **46**, 229–248.
McIntosh, T. J. (1978). *Biochim. Biophys. Acta*, **513**, 43–58.
Nagle, J. F. & Wilkinson, D. A. (1978). *Biophys J.* **23**, 159–175.
Nicholson, L. K. & Cross, T. A. (1989). *Biochemistry*, **28**, 9379–9385.
Olah, G. A. (1990). Ph.D. thesis, Rice University, Houston, TX.
Olah, G. A. & Huang, H. W. (1988). *J. Chem. Phys.* **89**, 2531–2538.
Parsegian, A. (1969). *Nature (London)*, **221**, 844–846.
Perutz, M. F. (1954). *Proc. Roy. Soc. ser A*, **225**, 264–286.
Pullman, A. (1987). *Quart. Rev. Biophys.* **20**, 173–200.
Rand, R. P. & Pangborn, W. A. (1973). *Biochim. Biophys. Acta*, **318**, 299–305.
Roux, B. & Karplus, M. (1988). *Biophys J.* **53**, 297–309.
Saxena, A. M. & Schoenborn, B. P. (1977). *Acta. Crystallogr. sect. A*, **33**, 813–818.
Shannon, C. E. (1949). *Proc. Inst. Radio Eng. N.Y.* **37**, 10–21.
Torbet, J. & Wilkins, M. H. F. (1976). *J. Theoret. Biol.* **62**, 447–458.
Urry, D. W. (1985). In *Enzymes of Biological Membranes* (Martonosi, A. N., ed.), vol. 1, pp. 229–258, Plenum Publishing, New York.
Urry, D. W., Spisni, A. & Khaled, M. A. (1979). *Biochem. Biophys. Res. Commun.* **88**, 940–949.
Urry, D. W., Jing, N., Trapane, T. L., Luan, C.-H. & Waller, M. (1988). In *Current Topics in Membranes and Transport* (Hoffman, J. F. & Giebisch, G., ed.), vol. 33, pp. 51–90, Academic Press, New York.
Wallace, B. A. & Ravikumar, K. (1988). *Science*, **241**, 182–187.
Worcester, D. L. & Franks, N. P. (1976). *J. Mol. Biol.* **100**, 359–378.
Wu, Y., Huang, H. W. & Olah, G. A. (1990). *Biophys. J.* **57**, 797–806.

Edited by R. Huber